AD-A037 165 AIR FORCE MATERIALS LAB WRIGHT-PATTERSON AFB OHIO F/G 11/2
IMPACT RESISTANCE OF STRUCTURAL CERAMICS. PART II. BALLISTIC TE--ETC(U)
DEC 76 J M WIMMER, I BRANSKY, N M TALLAN

UNCLASSIFIED AFML-TR-76-56-PT-2 NL

1 OF 1
AD A037165

END

DATE FILMED
4-77

AFML-TR-76-56
Part II

(12)

IMPACT RESISTANCE OF STRUCTURAL CERAMICS

Part II:
BALLISTIC TESTS

PROCESSING AND HIGH TEMPERATURE MATERIALS BRANCH
METALS AND CERAMICS DIVISION

DECEMBER 1976

TECHNICAL REPORT AFML-TR-76-56, Part II
FINAL REPORT FOR PERIOD JUNE 1975 - FEBRUARY 1976

AIR FORCE MATERIALS LABORATORY
AIR FORCE WRIGHT AERONAUTICAL LABORATORIES
AIR FORCE SYSTEMS COMMAND
WRIGHT-PATTERSON AIR FORCE BASE, OHIO 45433

NOTICE

When Government drawings, specifications, or other data are used for any purpose other than in connection with a definitely related Government procurement operation, the United States Government thereby incurs no responsibility nor any obligation whatsoever; and the fact that the government may have formulated, furnished, or in any way supplied the said drawings, specifications, or other data, is not to be regarded by implication or otherwise as in any manner licensing the holder or any other person or corporation, or conveying any rights or permission to manufacture, use, or sell any patented invention that may in any way be related thereto.

This report has been reviewed by the Information Office (OI) and is releasable to the National Technical Information Service (NTIS). At NTIS, it will be available to the general public, including foriegn nations.

This technical report has been reviewed and is approved for publication.

JAMES M. WIMMER
Project Scientist

FOR THE COMMANDER

NORMAN M. TALLAN
Acting Chief, Processing and High
Temperature Materials Branch
Metals and Ceramics Division
Air Force Materials Laboratory

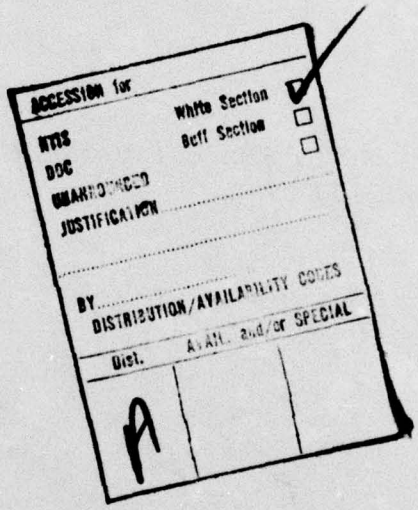

Copies of this report should not be returned unless return is required by security considerations, contractual obligations, or notice on a specific document.

UNCLASSIFIED

SECURITY CLASSIFICATION OF THIS PAGE *(When Data Entered)*

REPORT DOCUMENTATION PAGE

READ INSTRUCTIONS BEFORE COMPLETING FORM

1. REPORT NUMBER: AFML-TR-76-56, Part II
2. GOVT ACCESSION NO.
3. RECIPIENT'S CATALOG NUMBER
4. TITLE *(and Subtitle)*: IMPACT RESISTANCE OF STRUCTURAL CERAMICS. PART II. BALLISTIC TESTS.
5. TYPE OF REPORT & PERIOD COVERED: Final Report. Jun 75 — Feb 76
6. PERFORMING ORG. REPORT NUMBER
7. AUTHOR(s): M. Wimmer, I. Bransky, M. Tallan (Norman)
8. CONTRACT OR GRANT NUMBER(s): AD-A030 878
9. PERFORMING ORGANIZATION NAME AND ADDRESS: Processing and High Temperature Materials Branch, Metals and Ceramics Division, Air Force Materials Laboratory, WPAFB, Ohio
10. PROGRAM ELEMENT, PROJECT, TASK AREA & WORK UNIT NUMBERS: 61102F, 70210273, 42
11. CONTROLLING OFFICE NAME AND ADDRESS: Same
12. REPORT DATE: Dec 76
13. NUMBER OF PAGES: 42 (42 p.)
14. MONITORING AGENCY NAME & ADDRESS *(if different from Controlling Office)*
15. SECURITY CLASS. *(of this report)*: UNCLASSIFIED
15a. DECLASSIFICATION/DOWNGRADING SCHEDULE

16. DISTRIBUTION STATEMENT *(of this Report)*

Approved for public release; distribution unlimited.

17. DISTRIBUTION STATEMENT *(of the abstract entered in Block 20, if different from Report)*

18. SUPPLEMENTARY NOTES

AD-A030 878

19. KEY WORDS *(Continue on reverse side if necessary and identify by block number)*

Ceramics
Impact Resistance
Silicon Nitride
Silicon Carbide
Aluminum Oxide
Dynamic Strength
Hertzian Damage

20. ABSTRACT *(Continue on reverse side if necessary and identify by block number)*

Two mechanisms can lead to failure of ceramics under impact, (1) failure due to flexural stresses, and (2) failure due to Hertzian type cracks introduced locally by the impactor. These mechanisms have been studied in silicon nitride, silicon carbide, and aluminum oxide ceramics using 200-1000 f/s BB ball steel impactors and different types of specimen support. The critical velocities for flexural failure and Hertzian damage of 1 x 1 x 0.2 inch plates were determined.

DD FORM 1 JAN 73 1473 EDITION OF 1 NOV 65 IS OBSOLETE

UNCLASSIFIED

SECURITY CLASSIFICATION OF THIS PAGE *(When Data Entered)*

012 320

FOREWORD

This report was prepared by the Processing and High-Temperature Materials Branch, Metals and Ceramics Division, Air Force Materials Laboratory, Wright-Patterson Air Force Base, Ohio. The research reported on covered time period from June 1975 to February 1976 while Dr. I. Bransky was working in the AFML as a Visiting Scientist under Contract F33615-73-C-4155 held by Technology, Inc., Dayton, Ohio. Dr. Bransky is permanently employed by Israel's Ministry of Defense. Dr. J. M. Wimmer (AFML/LLM) was the government Project Scientist. Much of the work was carried out in the AFML Impact Mechanics Laboratory and their outstanding cooperation is gratefully acknowledged. This report was submitted 20 June 1976.

TABLE OF CONTENTS

LIST OF ILLUSTRATIONS

LIST OF ILLUSTRATIONS (Cont'd)

LIST OF TABLES

SECTION I

INTRODUCTION

The purpose of the ballistic tests was to compare the impact resistance of several ceramics which are candidates for application in high-temperature gas turbine engines. One type of test allowed the simultaneous generation of both flexural and localized contact stresses and for the specimen sizes used, failure was usually due to flexural stresses. The other type of test allowed only localized contact stresses and in this case failure or strength degradation was due to Hertzian cracking.

It was not intended here to study particular ceramic component design configurations but rather to gain some general understanding of the type of damage caused by a small, high velocity impactor. As expected, this damage was found to depend not only on the inherent properties of the ceramics tested but also on specimen thickness and the type of support. In addition to room temperature tests, some experiments were carried out at 1300°C, close to the expected service temperature in the turbine application.

From the results of these experiments some conclusions can be derived concerning the relative ballistic impact strength, i.e., the relative resistance to foreign object damage of the ceramics tested and potential ways of increasing this impact strength.

SECTION II

EXPERIMENTAL PROCEDURES

High velocity impact tests were carried out on hot-pressed Si_3N_4 (NC-132),* reaction bonded Si_3N_4 (NC-350),* hot-pressed SiC (NC-203),* and sintered alumina (AD998).† The specimens were in the form of 1" square plates 0.1 - 0.2" thick. A smooth bore gun ‡ powered with compressed nitrogen was used to drive 0.177" dia., 3.5 g steel BB balls at velocities up to 1000 f/s. The velocity of the ball prior to impact was determined from the time of flight between two parallel laser beams perpendicular to the ball trajectory.

Two types of specimen support were employed. (1) Anvil Support - in this case the back side of the specimen was fully supported by an alumina rod, 2" in diameter and 1.5" long. The specimen was pressed firmly against the polished end of the rod which contacted a massive steel support. At room temperature a thin layer of vacuum grease was applied between the sample and the anvil to assure good acoustic contact. (2) Ring Support - this support consisted of an alumina ring 1.18" I.D. and 1.4" O.D.. Here, the specimen was supported at the four corners and the impact loading at the center of the plate developed flexural stresses in addition to the localized force at the point of impact. Both types of specimen support could be inserted into a horizontal tube furnace for ballistic tests up to 1300°C.

*Norton Co., Worcester, Mass.

†Coors Porcelain Co., Golden, Colo.

‡Air Force Materials Laboratory (LLN) Impact Mechanics Facility, WPAFB, Ohio.

SECTION III

RESULTS

1. PRELIMINARY TESTS ON Al_2O_3 (AD998)

Although alumina is not being seriously considered as a candidate for high-temperature turbine components, it was included in this study so that initial test experience could be obtained with an inexpensive material and for purposes of comparison. Twenty-five specimens, 1 x 1 x 0.2 inches, were impacted at room temperature and at 1300°C using the ring support. The following results were obtained:

a. Up to a velocity of about 230 f/s no visible damage was observed.

b. Above 270 - 310 f/s at room temperature most of the specimens fractured into four squares as shown in Figure 1.

c. In the velocity range from 230 to 270 f/s the specimens did not visibly fracture. However, the use of a dye penetrant* indicated that these specimens contained a number of cracks as indicated in Figure 2.

d. On inspecting the fractured specimens it appeared that failure was due to either of two mechanisms, localized Hertzian cracking or flexural stresses. The first case is illustrated in Figure 3 where it appears that a Hertzian cone crack initiated at the point of impact. In the second case fracture originated in most cases at the center of a specimen edge such as illustrated in Figure 4.

e. An increase of about 20 f/s in the critical velocity, † i.e., not more than 10%, was observed for specimens impacted at 1300°C.

f The critical velocity for a 0.1" thick plate was found to be about 70 f/s. Therefore, it is estimated that the dependence of the critical velocity, v_c, on specimen thickness is $v_c \sim t^2$.

*Magnaflux Co., Type SK-3.

†The critical velocity is the velocity at which 50% of the specimens fracture into two or more pieces.

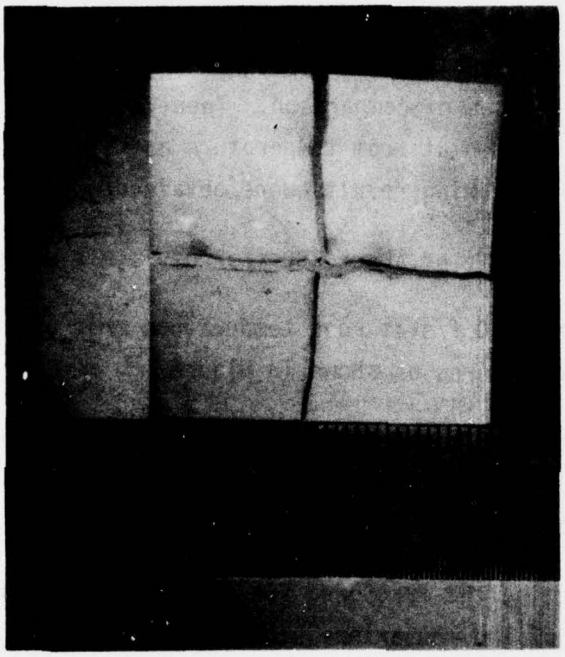

Figure 1. Flexural Fracture, 0.2" Thick Al_2O_3 (AD998), Ring Support, 370 f/s

2a. Impact Face

2b. Back Face

Figure 2. Flexural Cracks, 0.2" Thick Al_2O_3 (AD998), Ring Support, 250 f/s, (a) Impact Face, (b) Back Face (Impactor shown also)

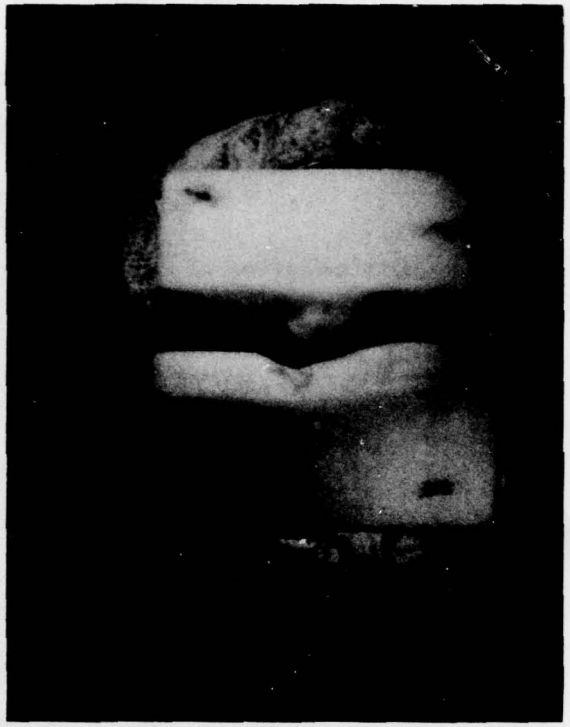

3a. Impact Face

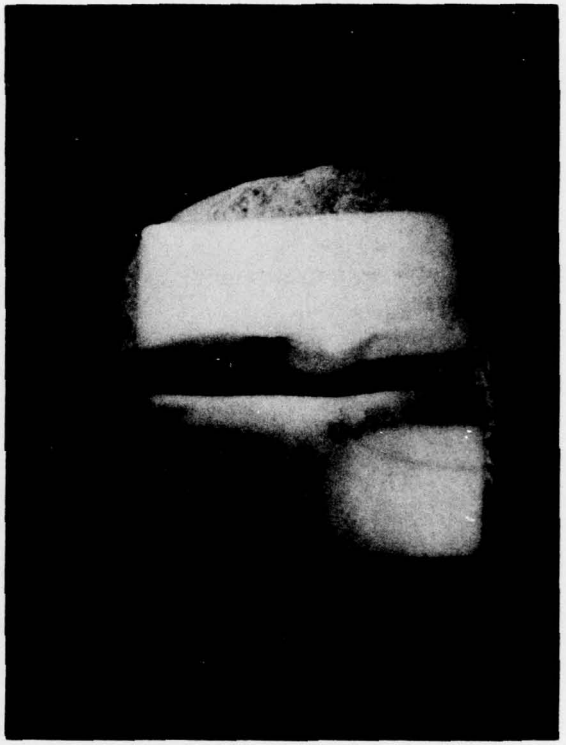

3b. Back Face

Figure 3. Hertzian Crack, 0.2" Thick Al_2O_3 (AD998), Ring Support, 280 f/s, (a) Impact Face, (b) Back Face

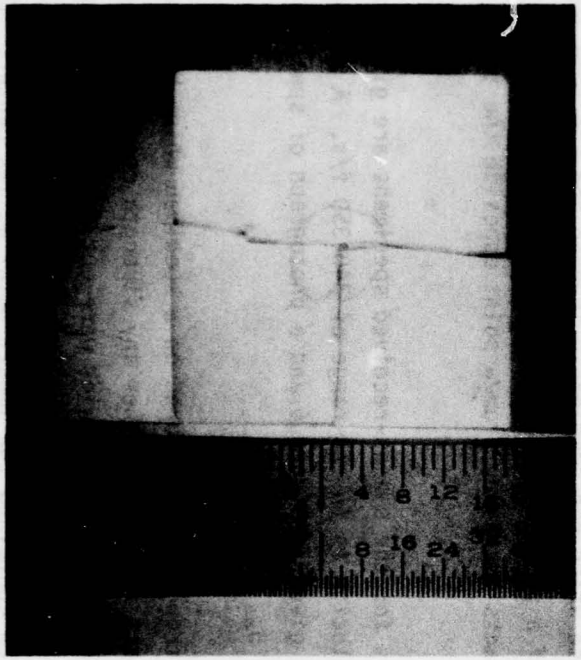

4a. Impact Face

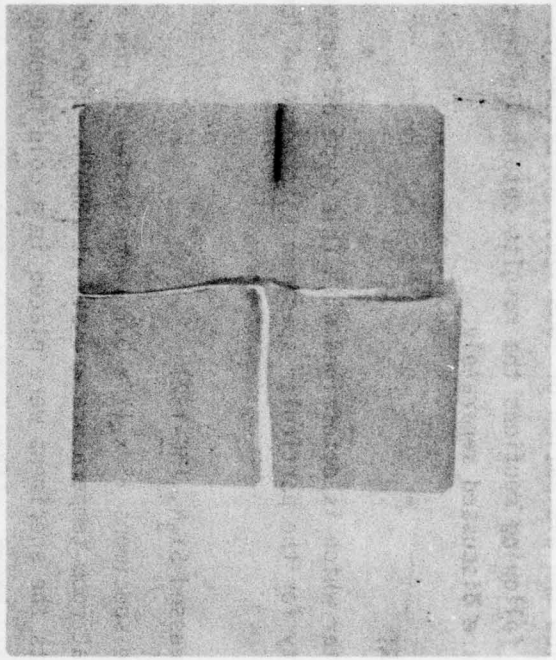

4b. Back Face

Figure 4. Flexural Cracks, 0.2" Thick Al_2O_3 (AD998), Ring Support, 332 f/s, (a) Impact Face, (b) Back Face (Note edge crack revealed by dye penetrant)

Following these preliminary tests it was decided to use two types of specimen support one of which, the anvil support, would eliminate flexural stresses and allow the evaluation of localized, Hertzian-type impact damage. In the following sections the results obtained with the ring and anvil supports are discussed separately.

2. RING SUPPORT

The parameter which is determined with this type of support is the critical velocity for the particular specimen thickness and impactor used.

a. Hot-Pressed Si_3N_4 (NC-132)

Twelve specimens 1" x 1" x 0.2" were tested in the as-received condition, six at room temperature and six at 1300°C. For the high-temperature tests the specimens were placed in a cold furnace and heated to 1300°C in 1-1/2 hours. After impact the specimens were inspected for cracks using a fluorescent dye penetrant.* Unlike alumina, hot-pressed Si_3N_4 showed no visible damage until catastrophic fracture occurred. At that point a number of cracks could be observed by the dye penetrant in addition to those which ran completely through the specimen. Figure 5 is an example of a plate which broke into four pieces on impact. A number of secondary cracks emanating from a point opposite the impact are also observed.

The results for the six as-received specimens are given in Table 1. The critical velocity is in the range of 340-350 f/s. A photograph of specimen 103 is given in Figure 6 and a photograph of specimen 104 is given in Figure 5.

Residual strength was measured on a specimen which had received a subcritical impact to check whether any strength degradation occurred. For this purpose, two bars 0.2" wide were cut from specimen 102 and their unimpacted face was diamond ground, thus ending with test bars 1" x 0.2" x 0.1" one of which contained the impact point at its center. The bars

*Zyglo, Magnaflux Co., Type ZL-22A.

TABLE 1

IMPACT RESULTS FOR AS-RECEIVED Si_3N_4 (NC-132)
AT ROOM TEMPERATURE (RING SUPPORT, SINGLE IMPACT)

Specimen No.	Ball Velocity (f/s)	Impact Damage
100	283	no visible damage
101	315	" " "
102	322	" " "
103	340	corner chipped
104	356	fractured into four pieces
105	414	fractured into six pieces

*Magnaflux Co., Type SK-3.

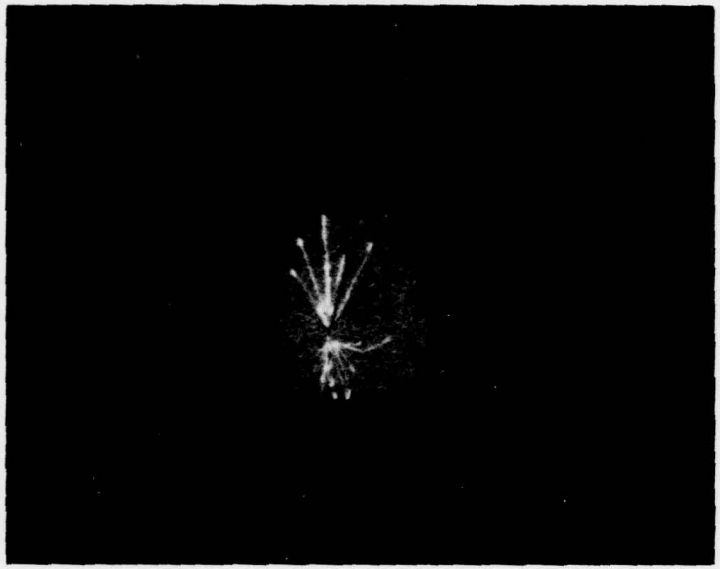

Figure 5. Flexural Cracks, 0.2" Thick Si_3N_4 (NC-132), Ring Support, 356 f/s, Back Face (Zyglo dye penetrant)

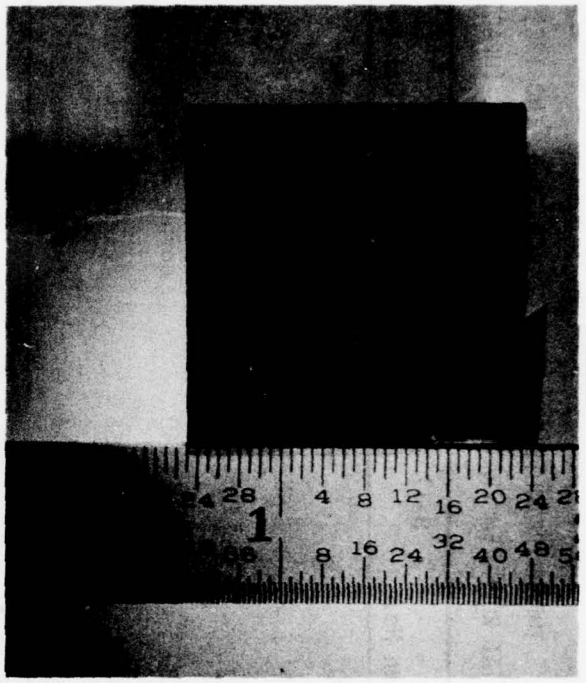

Figure 6. Flexural Failure, 0.2" Thick Si_3N_4 (NC-132) Ring Support, 340 f/s, Impact Face, Specimen No. 103, Impact Area Circled

were tested in four-point bending using a 3/8" span. The bar which contained the impact point was placed so that the impact point was on the tensile side of the bend bar. This bar had a strength of 545 MN/m^2 while the bar to the side of the point of impact had a fracture strength of 540 MN/m^2 indicating that no cracks were produced until the plate visibly fractured.

The results for the six bars impacted at 1300°C are given in Table 2. At this temperature no damage was observed up to 484 f/s. Two bars cut from specimen 111 had residual strengths of 548 and 511 MN/m^2, the latter value for the bar containing the impact point on the tensile side.

TABLE 2

IMPACT RESULTS FOR AS-RECEIVED Si_3N_4 (NC-132)
AT 1300°C (RING SUPPORT, SINGLE IMPACT)

Specimen No.	Ball Velocity (f/s)	Impact Damage
106	315	no visible damage
107	364	" " "
108	387	" " "
109	393	" " "
110	441	" " "
111	484	" " "

It might at first appear from these results that NC-132 is much more impact resistance at high-temperature. However, when specimen 107 was subsequently impacted at room temperature complete fracture did not occur until a velocity of 500 f/s was attained. A second specimen, No. 108, sustained a total of 11 room temperature impacts between 180 f/s and 515 f/s where fracture occurred. The velocity at which fracture occurred in these specimens is considerably higher than the critical velocity obtained on as-received specimens and indicates that the improvement of impact resistance at high-temperature is not due to

a change in material properties such as an increase in K_{IC}, but is due to the effect of the high-temperature and environment on the nature of the surface or edge flaws. Two additional specimens of NC-132 were annealed at 1400°C for one hour in air and then impacted at room temperature. One specimen fractured at 493 f/s while a corner of the second chipped off at 516 f/s. Therefore, it appears that for the specimen dimensions and type of impactor used the critical velocity for annealed specimens is about 500 f/s at room temperature. Since K_{IC} does not increase significantly at high-temperatures under rapid loading conditions[1] the critical velocity would not be expected to be significantly (<20%) higher at 1300°C.

b. Hot-Pressed SiC (NC-203)

Eight specimens of NC-203 were tested in the ring support at room temperature after annealing at 1350°C for one hour. Initial results on six of these specimens indicated that the critical velocity was below 250 f/s. However, when the edges of the specimens were beveled with 240 grit SiC paper the critical velocity appeared to be in the range of 400 f/s. The results on these specimens are given in Table 3.

TABLE 3

IMPACT RESULTS FOR SiC (NC-203) AT ROOM TEMPERATURE WITH RING SUPPORT

Specimen No.	Ball Velocity (f/s)	Impact Damage	Comments
8081	247	2 corners broke off	
8082	140	no visible damage	
8083	215	broke into 4 pieces	impacted off center
8084	180	no visible damage	
	210	no visible damage	
8086	227	corner broke off	
8087	367	broke into 5 pieces	
8088	251	no visible damage	edges beveled
	354	no visible damage	
	431	corner broke off	
8091	356	no visible damage	edges beveled
	408	corner broke off	

c. Reaction Bonded Si_3N_4 (NC-350)

These specimens were only 0.125" thick and therefore no direct comparison with the 0.2" thick specimens of other materials can be made. In addition, the low fracture velocity (<100 f/s) in the ring support made it impossible to determine the critical value since the air gun could not be controlled at such low velocities. Figure 7 shows the type of fracture that was observed at 1300°C.

3. ANVIL SUPPORT

The approach taken with this type of support was to increase the impactor velocity until fracture occurred and then to impact a number of specimens over a range of subcritical velocities. The fracture strength of test bars cut from these specimens and containing the impact point was then measured to determine if any strength degradation occurred.

a. Hot-Pressed Si_3N_4 (NC-132)

The first batch of five specimens (1" x 1" x 0.2" plates) were annealed in air at 1300°C for one hour and then impacted at room temperature. The results are given in Table 4, and indicate that the specimens did not visibly fracture up to 825 f/s.

Following these initial tests a second group of annealed specimens was impacted to check for strength degradation. In some cases the specimen and support were repositioned after each impact so that three test bars, each containing a single impact point, could be cut from one plate. The results are given in Table 5.

Specimen 121 failed on impact and as shown in Figure 8 a cone was clearly visible on the fracture surface indicating that failure due to a Hertzian-type stress pattern was responsible for failure. In the two specimens with the lowest residual strength, (122 and 123), Hertzian cracks appear to extend to a depth which is 80% of the specimen thickness. The fracture surfaces of these specimens are illustrated in Figure 9. Even though several other specimens failed at the point of impact, definite

7a. 187 f/s

7b. 184 f/s

Figure 7. Flexural Failure, 0.125" Thick Si_3N_4 (NC-350) Ring Support, 1300°C Back Face, (a) 187 f/s, (b) 184 f/s

TABLE 4

RESULTS FOR MULTIPLE ROOM TEMPERATURE IMPACT OF Si_3N_4 (NC-132) WITH ANVIL SUPPORT

Specimen No.	Ball Velocity (f/s)	Comments
112	224	no visible damage
	351	" " "
	435	fractured*
113	467	no visible damage
	424	" " "
	437	" " "
	428	" " "
114	413	no visible damage
	450	" " "
	540	" " "
115	350	no visible damage
	674	" " "
	765	" " "
	825	" " "
116	687	no visible damage
	738	" " "
	822	" " "

*No grease was applied in this test between specimen and support.

TABLE 5

RESIDUAL STRENGTH AFTER ROOM TEMPERATURE IMPACT OF Si_3N_4 (NC-132) WITH ANVIL SUPPORT

Specimen No.	Ball Velocity (f/s)	σ_f(MN/m^2)	Comments
117	473	585	failed at impact point
118	490	473	did not fail at impact point
119	650	371	failed 3 mm to side of impact
120	758	359	failed at impact point
121	839	-	Hertzian fracture on impact
122	926	304	visible cone crack
123	825	271	visible cone crack
	765	376	failed at impact point
124	450	489	failed at edge
125	401	634	" " "
	396	443	" " "
	401	489	" " "
126	526	537	" " "
	526	526	failed at impact point
	495	590	" " "
127	602	449	failed at edge
	600	594	" " "
	594	645	failed at impact point
128	679	682	failed at edge
	688	572	failed at impact point
	690	446	" " "

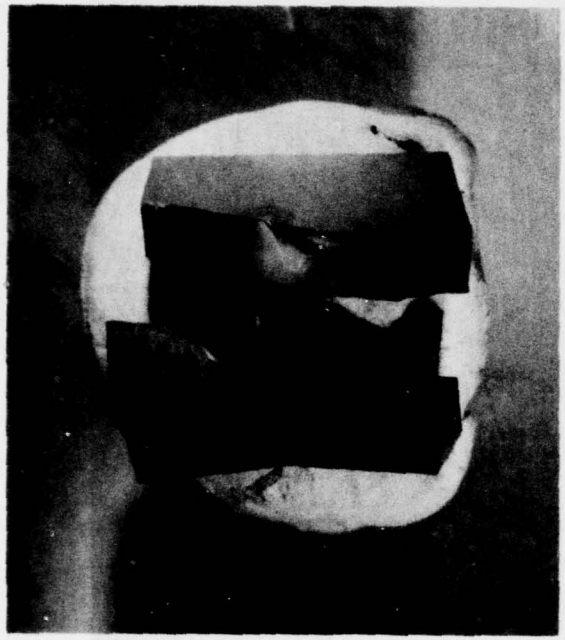

8a. Impact Face

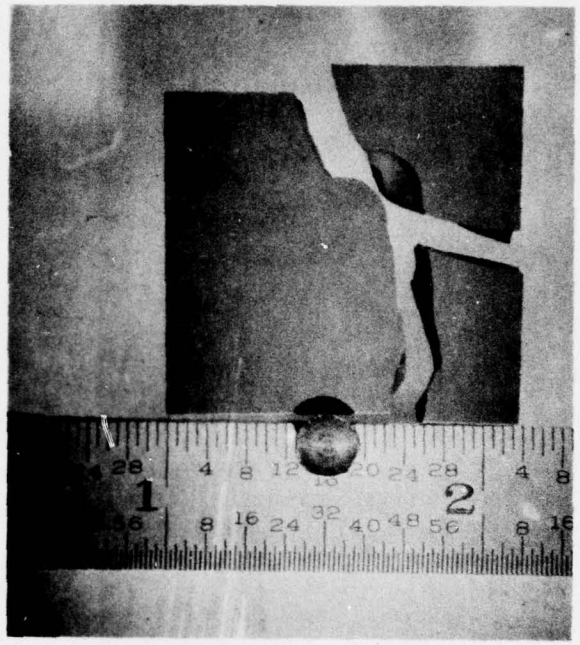

8b. Back Face

Figure 8. Hertzian Cone Crack, 0.2" Thick Si_3N_4 (NC-132), Anvil Support, 839 f/s, (a) Impact Face, (b) Back Face (Deformed impactor shown)

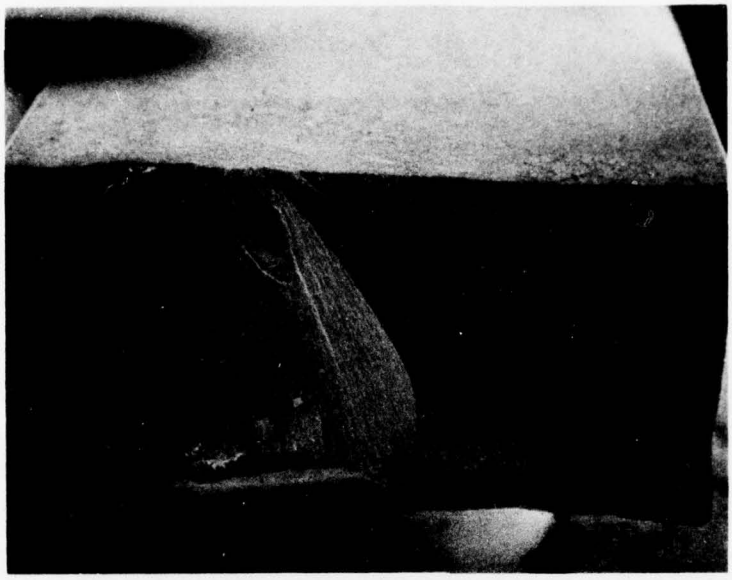

9a. 926 f/s

9b. 825 f/s

Figure 9. Hertzian Cone Crack on Fracture Surface of 0.1" Thick Bend Bar, Si_3N_4 (NC-132), Anvil Support, (a) 926 f/s, (b) 825 f/s

Hertzian cracks were not apparent on the fracture surface, two examples of which are shown in Figure 10. In these cases the area where fracture initiated has the appearance of a fracture mirror with a radius of the order of 100 μ.

b. Hot-Pressed SiC (NC-203)

A total of 11 1" x 1" x 0.2" annealed specimens were impacted at room temperature. At subcritical velocities each plate was impacted three times, in the center and to each side of center, so that three bars, each containing an impact point, could be cut from the plate for residual strength measurements. These bars were 1" x 0.2" x 0.1" thick. The results are given in Table 6.

The Hertzian fracture of specimen 8098 showing a complete cone is shown in Figure 11. Partial cone cracks were visible on the fracture surface of several of the bars used for residual strengtn. Examples are given in Figure 12 for specimens impacted at 667, 698, and 585 f/s. Below 400 f/s none of the residual strength bars failed at the point of impact.

c. Reaction-Bonded Si_3N_4 (NC-350)

Six specimens 1" x 1" x 0.125" were impacted at room temperature in the as-received condition. Since this material has a surface layer, 150 - 200 μ thick, which appears lighter than the bulk material it was decided that the whole plate should be tested for residual strength without cutting out test bars. Therefore, a test jig similar to that described by Wachtman (Reference 2) was constructed. The plate was supported on three 0.125" ball bearings on a 0.4" radius circle. The load was applied to the center of the plate through a drill rod with a 0.612" diameter flat tip. The equations given in Reference 2 were used to calculate the strength. Although these were derived for a circular specimen it does not appear that their use on square plates would cause a large error since the circle of support was completely within the square plate. A specimen radius of 0.5" was used in the calculations. The results are given in Table 7.

10a. 495 f/s

10b. 594 f/s

Figure 10. Fracture Surface of Residual Strength Bars Showing Critical Flaw Site, Si_3N_4 (NC-132), (a) 495 f/s, (b) 594 f/s (Specimen Nos. 126 and 127)

TABLE 6

RESIDUAL STRENGTH AFTER ROOM TEMPERATURE IMPACT OF SiC (NC-203) WITH ANVIL SUPPORT

Specimen No.	Ball Velocity (f/s)	σ_f(MN/m^2)	Comments
8093	667	140	visible cone crack
	629	306	failed at impact point
8097	774	-	Hertzian fracture on impact
8098	774	-	Hertzian fracture on impact
8099	848	-	Hertzian fracture on impact
8101	698	370	visible cone crack
	703	333	failed at impact point
	688	338	visible cone crack
8104	579	676	failed at impact point
	585	329	" " " "
8107	526	329	did not fail at impact point
	522	524	did not fail at impact point
	522	586	did not fail at impact point
8111	454	383	possibly failed at impact point
	452	545	did not fail at impact point
	457	402	probably failed at impact point
8114	393	504	did not fail at impact point
	397	531	did not fail at impact point
	381	470	did not fail at impact point
8117	358	483	did not fail at impact point
	356	630	did not fail at impact point
	356	534	did not fail at impact point

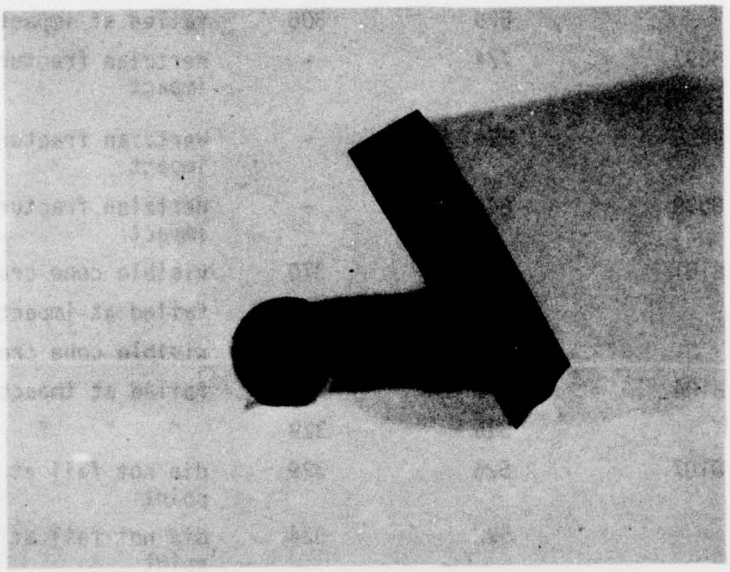

Figure 11. Hertzian Cone Crack, 0.2" Thick SiC (NC-203), Anvil Support, 774 f/s

12a. 667 f/s

12b. 698 f/s

12c. 585 f/s

Figure 12. Fracture Surface of Residual Strength Bars, SiC (NC-203), (a) 667 f/s, (b) 698 f/s, (c) 585 f/s

TABLE 7

RESIDUAL STRENGTH AFTER ROOM TEMPERATURE IMPACT OF Si_3N_4 (NC-350) WITH ANVIL SUPPORT

Specimen No.	Ball Velocity (f/s)	σ_f(MN/m^2)	Comments
8026	123, 229, 355	-	complete fracture after 3rd hit
8032	157	0	no visible fracture on impact but broke immediately on loading
8029	163	221	broke into 4 pieces
8033	196	11	broke into 3 pieces
8030	226	-	fractured on impact
8031	226	-	" " "

Three virgin plates were tested for static strength giving the results 226, 237, and 219 MN/m^2. Figure 13 gives an example of a complete fracture at 226 f/s.

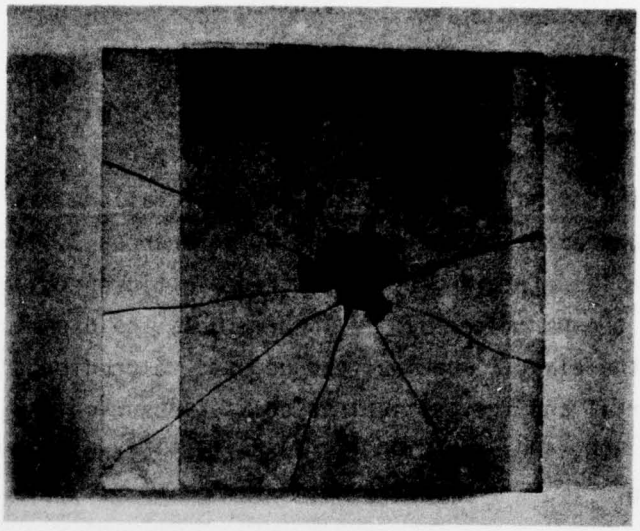

13a. Impact Face

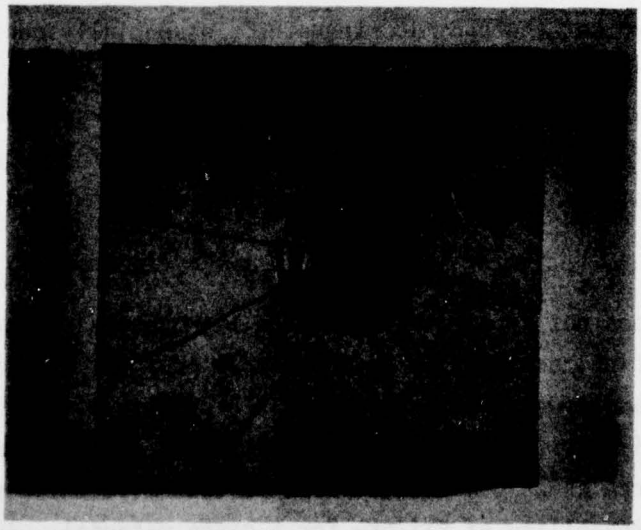

13b. Back Face

Figure 13. Hertzian Failure, 0.1" Thick Si_3N_4 (NC-350) Anvil Support, 226 f/s, (a) Impact Face, (b) Back Face

SECTION IV

DISCUSSION

1. RING SUPPORT

For this type of support the onset of failure was due to flexural stresses and as discussed previously (References 3, 4) the impact resistance is determined by the stored elastic energy at fracture. In this case the parameter σ_{dyn}^2/E, where σ is the dynamic fracture stress and E is the elastic modulus, can be used to predict the impact resistance of a material and the critical velocities observed for NC-132, NC-203, and NC-350 of 500, 400, and <100 f/s respectively are in agreement with this prediction.

Although the experimental data for the ballistic tests are not very extensive there does not appear to be a strong effect of temperature on the impact resistance. The elastic modulus decreases somewhat with temperature but the dynamic strength is essentially constant since under these rapid loading conditions K_{IC} is practically temperature independent (Reference 1) even for NC-132. There is, of course, usually some environmental effect which can be beneficial in terms of flaw healing and residual stress relief but which can also degrade the strength in some materials.

It does not appear that any more than general comments can be made from the ring test results as they apply only for the specific specimen geometry and type of impactor used. In principle, the impactor characteristics (mass, radius, velocity, etc.) can be converted to an impact force which can then be used to determine the resulting stress and the probability of failure for a given material. Such analyses are available for elastic impacts but the steel balls used in the present study visibly deformed on impact making the analysis much more difficult. However, one can conclude that since the dimensions of the specimens used are about what one would expect for small ceramic turbine vanes and blades that failure due to metal impactors the size of BB balls would usually occur due to flexural stresses rather than Hertzian damage since as observed above Hertzian damage occurs at significantly higher velocities.

2. ANVIL SUPPORT

For this type of support only failure due to Hertzian-type damage was observed. Again, relatively simple analyses are available for purely elastic impacts but not for the case where the impactor deforms. Therefore, the velocities at which Hertzian cone cracks were observed are only valid for the type of impactor used. Hertzian fracture has been discussed by a number of authors (References 5, 6, 7). For the case of a spherical indentor the geometry is illustrated in Figure 14.

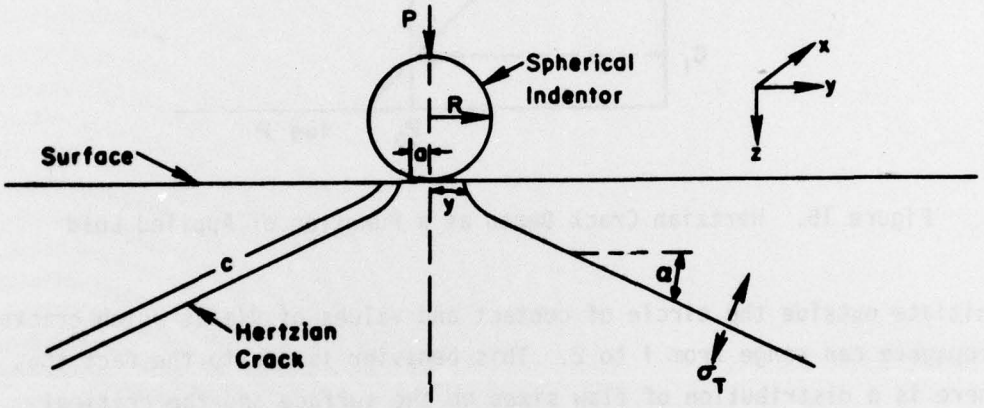

Figure 14. Hertzian Crack Due to Spherical Indentor

where R = indentor radius, a = radius of contact, and σ_T = largest principle tensile stress. For large Hertzian cracks, $\alpha \approx 22°$ (Reference 5). The relation between the applied force, P, and the Hertzian crack size, C, is illustrated in Figure 15 (References 5, 6, 7). For $C<C_1$ the force required for crack extension decreases with increasing crack size so that in this region the crack is unstable. For $C>C_2$ the force required for crack extension increases as the crack size increases so the crack is stable. If the initial flaw size in the material is C_i then a force P_o will be required for crack extension which will continue until the crack length reaches C_o. Referring back to Figure 14, the maximum tensile stress at the surface is on the circle of contact, i.e., at y = a, and falls off along outward radials. However, the initial Hertzian ring cracks are usually observed to have a larger radius indicating that they

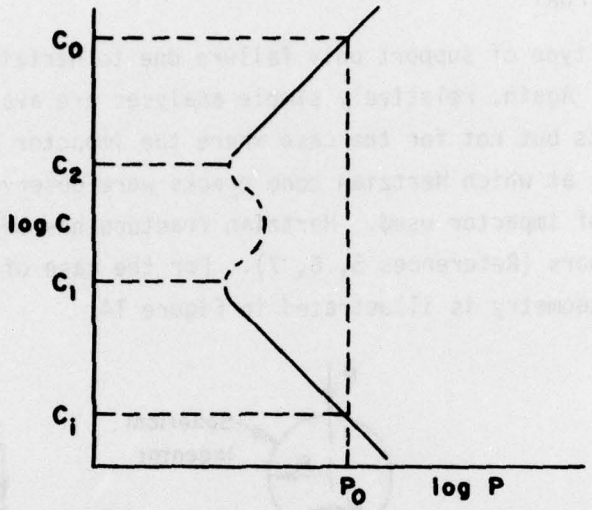

Figure 15. Hertzian Crack Depth as a Function of Applied Load

initiate outside the circle of contact and values of y/a at which cracks propagate can range from 1 to 2. This behavior is due to the fact that there is a distribution of flaw sizes on the surface and the critical flaw in the localized stress field will generally not be on the circle of contact especially for small radius indentors. The fact that $y/a > 1$ has also been used (Reference 6) to explain Auerbach's law which states that the critical load for Hertzian crack formation is proportional to the radius of the indentor for small indentors.

In dealing with the strength degradation problem one is initially concerned with the region below C_1 in Figure 15 where the critical load to propagate a crack of size C from a point y/a is given by (Reference 6)

$$P_c = 14.1 \frac{K_{IC}^3 k^2 R^2}{(1-2\nu)^3 E^2} \left[\frac{y}{a}\right]^6 \left[\frac{1}{C}\right]^{3/2} \qquad (1)$$

where K_{IC} = critical stress intensity factor, ν = Poisson's ratio, E = Young's modulus, and $k = \frac{9}{16}\{(1-\nu^2) + (1-\nu_I^2) E/E_I\}$

where the subscript I refers to the indentor. Equation 1 could be used to compare the resistance of materials to Hertzian cracking but the initial flaw size and the value of y/a are generally not known. For a given value of C and y/a the critical load can be calculated if the elastic constants and K_{IC} are known. However, the calculation is very sensitive to the value taken for Poisson's ratio, a parameter which is not known very accurately for the materials of interest. Experimentally it has been found that for static loading, the critical force for hot-pressed silicon nitride is about four times that of hot-pressed silicon carbide for both hard (Reference 8) and deformable indentors (Reference 9).

The results of the present study differ from the picture of Hertzian fracture outlined previously in several respects. First, the Hertzian cracks are observed to extend into the specimens at a much sharper angle than the 22° predicted, the observed angle being about 60° for both NC-132 and NC-203. Since the crack should extend along the plane of the principle tensile stress this result indicates that the stress field is different than expected which may be a result of the nonelastic nature of the impact. As the impactor deforms, material flaws outward from the center of contact creating additional tensile stresses on the surface around the center of impact. The second difference is that the cone crack appears to initiate under the deformed impactor rather than at its perimeter which might also be explained by the presence of additional tensile stresses due to the deformation of the impactor.

The effect of these Hertzian cracks on strength is not as great as one would intuitively expect. For example, in the case of NC-132, specimens 122 and 123 had residual strengths of about one-half the unimpacted strength even though the cone crack appeared to extend to a depth almost 80% of the test bar thickness (Figure 9). Failure from a Hertzian crack has not been explicitly analyzed. For the case of a perfectly formed cone crack of depth L the entire circular crack front lies in a plane at this depth and there is no sharp crack front which intersects the surface. If L is over half the specimen thickness then the crack front lies within the compressive zone of the bend bar which suggests that fracture probably

initiates at secondary cracks produced at the point of impact. A semi-circular surface crack having a radius of 165 μ and oriented normal to the tensile stress would reduce the bend strength to 300 $MN/m^{3/2}$. Essentially the same observation was made for NC-203, the 1 mm deep crack shown in Figure 12b only reducing the strength to 370 MN/m^2.

Both the static loading results (References 8, 9) and Equation 1 indicate that NC-203 is more susceptible to Hertzian damage than NC-132. This is substantiated qualitatively by the data in Tables 5 and 6 which is also shown in Figure 16 where the circled data points are those for which there was evidence on the fracture surface that the impact produced the critical flaw. However, there is neither a drastic reduction in strength due to the onset of damage nor a large difference between the two materials. However, it should be recalled that these specimens had been annealed for one hour at 1300°C prior to impact so that the properties of the oxide layer could determine in large part the susceptibility of the material to Hertzian damage.

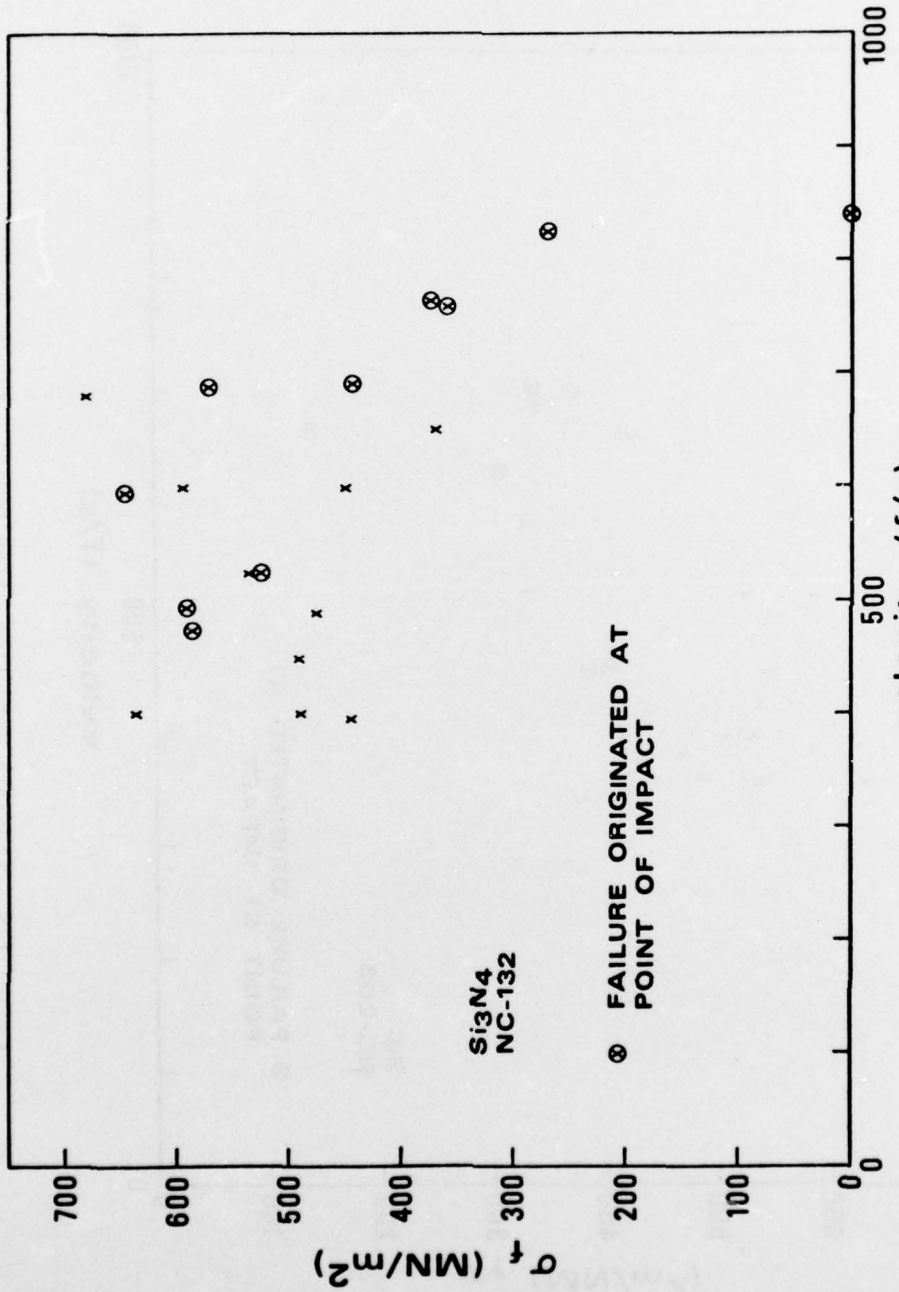

Figure 16a. Strength Retention After Impact, Si_3N_4 (NC-132)

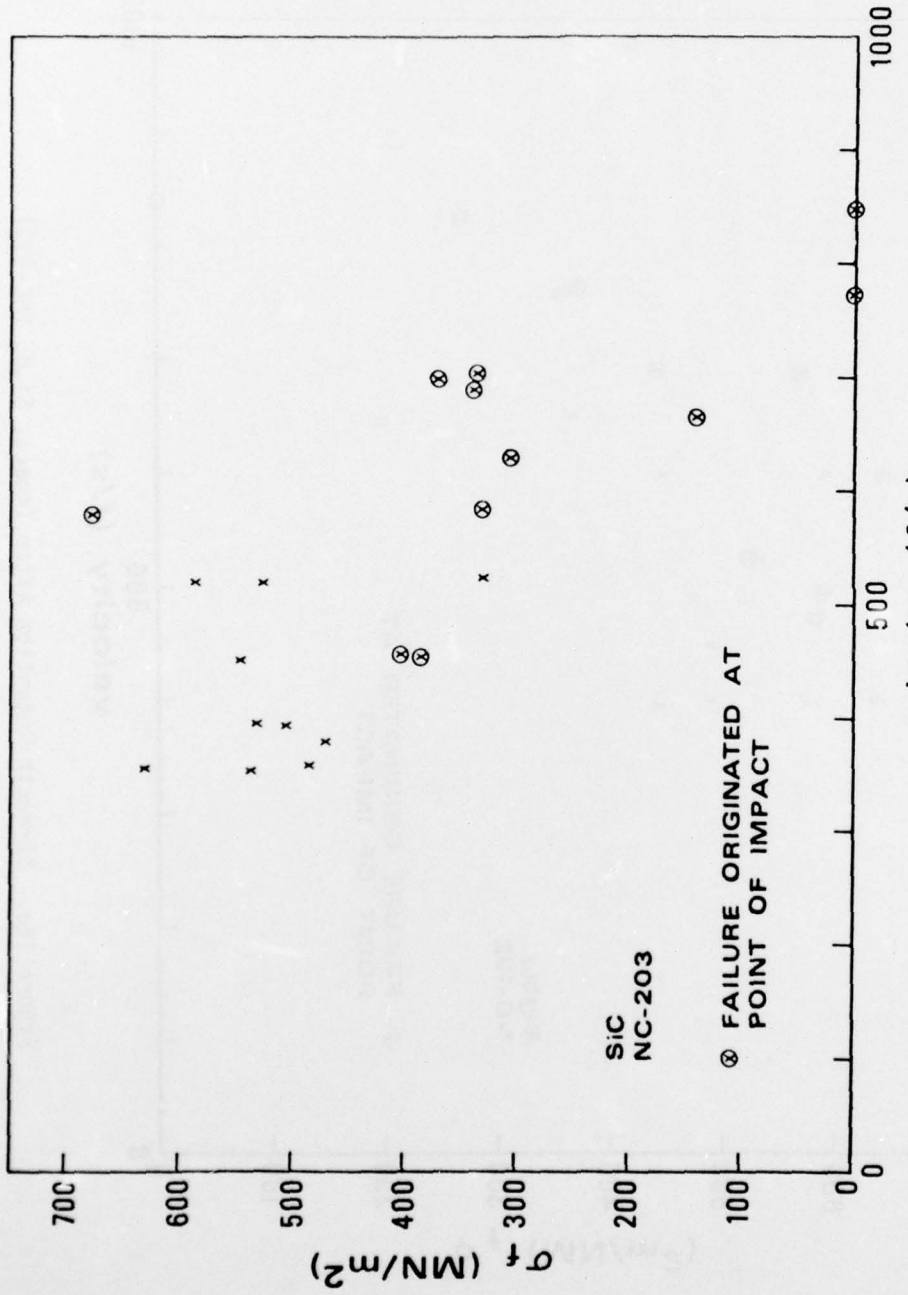

Figure 16b. Strength Retention After Impact, SiC (NC-203)

SECTION V

CONCLUSIONS

Under the impact conditions used two modes of failure were observed, flexural, and strength degradation due to Hertzian-type damage. The resistance of monolithic ceramics to flexural failure is essentially determined by the ability of the material to store energy elastically and in this respect NC-132 silicon nitride is superior. The classical picture of Hertzian crack formation for the case of static loading and as-machined surfaces does not appear to offer much insight to the practical case of deformable impactors striking oxidized surfaces as little difference was observed between hot-pressed silicon nitride and silicon carbide under these conditions. Although Hertzian cracks are observed which can cause catastrophic failure at high velocities, the onset of damage does not cause the degree of flexural strength degradation that might be expected. This is evidently due to the combination of crack geometry and test technique.

Resistance of a given material to flexural failure can be approached by increasing the materials strength but improvements greater than a factor of 3-4 can not realistically be expected. Therefore, decreasing the susceptibility of ceramics to flexural failure essentially becomes a design problem. Resistance to Hertzian damage is completely dependent on the state of the surface and therefore improvements such as energy absorbing layers (EAL's) have been shown (References 8, 10, 11) to offer a considerable increase in the impact resistance of dense silicon nitride and silicon carbide ceramics.

REFERENCES

1. M. G. Mendiratta, J. M. Wimmer, I. Bransky, "Determination of Dynamic Strength and K_{IC} of Hot-Pressed Si_3N_4," to be published in J. of Materials Science.

2. J. B. Wachtman, Jr., W. Copps, and J. Mandel, "Biaxial Flexure Tests of Ceramic Substrates," J. of Materials 7, 188 (1972).

3. R. W. Davidge and D. C. Phillips, "The Significance of Impact Data for Brittle Non-Metallic Materials," J. of Materials Science 7, 1308 (1972).

4. I. Bransky, J. M. Wimmer, N. M. Tallan, Impact Resistance of Structural Ceramics Part I: Instrumented Drop-Weight Tests," AFML-TR-76-56 Part I (1976).

5. F. C. Frank and B. R. Lawn, "On the Theory of Hertzian Fracture," Proc. Royal Society A, 299, 291 (1967).

6. T. R. Wilshaw, "Hertzian Fracture Test," J. Phys. D, 4, 1567 (1971).

7. A. G. Evans, "Strength Degradation by Projectile Impact," J. Am. Ceram. Soc., 56, 405 (1973).

8. H. P. Kirchner, R. M. Gruver, and C. S. Miller, "Localized Impact Damage in Ceramics," Tech. Report No. 3, ONR Contract No. N00014-74-C-0241 (January 1976).

9. F. F. Lange, "Relative Resistance of Dense Silicon Nitride and Silicon Carbide to Surface Damage Introduced by Hertzian Contact Stresses," Final Report, ONR Contract N00019-72-C-0278 (April 1973).

10. H. P. Kirchner and J. Seretsky, "Improving Impact Resistance by Energy-Absorbing Surface Layers," Ceramic Bulletin 54, 591 (1975).

11. J. A. Palm, "Improved Toughness of Silicon Carbide," Final Report on NASA Contract NAS3-17832 (January 1976).

☆ U. S. GOVERNMENT PRINTING OFFICE: 1977 — 757-001/230